THIS MONTH IN
JNM

Focus on the heart: Bengel provides an overview of promising techniques and potential challenges in cardiovascular molecular imaging to assess and predict disease, guide and monitor therapy, and translate novel approaches into routine clinical practice. . . . . ***Page 837***

Imaging CNS inflammation: Lopresti and Mason review current methods and tracers for assessing central nervous system inflammation and preview an article in this issue of *JNM* on the use of 2-^{18}F-fluoroacetate as an indicator of glial cell metabolism. . . . . ***Page 841***

Refining PET/CT in obese patients: Masuda and colleagues evaluate the effects of adjusting injected dose or acquisition time on the quality of ^{18}F-FDG PET/CT images of overweight patients. . . . . ***Page 844***

Thymic uptake of ^{18}F-FDG: Jerushalmi and colleagues characterize the incidence, patterns, and intensity of thymic ^{18}F-FDG uptake in relation to age and time elapsed after cancer treatment in a large cohort of patients. . . . . ***Page 849***

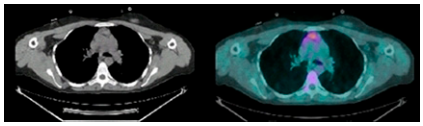

Timing vascular inflammation imaging: Menezes and colleagues report on studies to determine the ideal timing for PET/CT assessment of vascular uptake after injection of ^{18}F-FDG. . . . . ***Page 854***

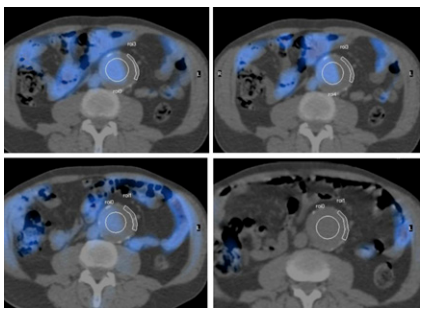

Prediction in neuroendocrine metastases: Garin and colleagues explore the utility of ^{18}F-FDG PET and somatostatin receptor scintigraphy in predicting early disease progression and survival in patients with metastatic neuroendocrine tumors. . . . . ***Page 858***

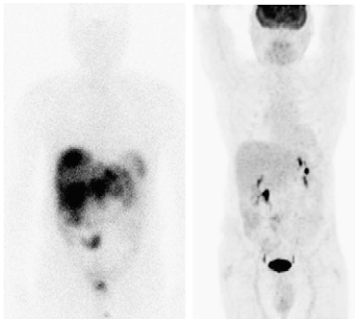

SPECT/CT in prostate cancer: Vermeeren and colleagues investigate the value of SPECT/CT for detection and anatomic localization of sentinel nodes before laparoscopic sentinel node lymphadenectomy in prostate carcinoma and compare the results with those from planar imaging. . . . . ***Page 865***

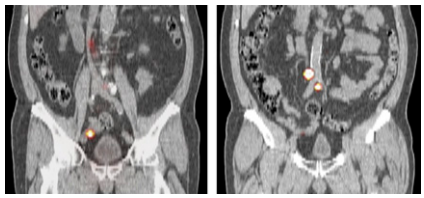

^{131}I-lipiodol in hepatocellular cancer: Marelli and colleagues compare the effects of ^{131}I-lipiodol treatment with those from transarterial chemoembolization or transarterial embolization in improving survival in patients with unresectable hepatocellular carcinoma. . . . . ***Page 871***

^{18}F-FDG and PiB in dementia: Lowe and colleagues evaluate the comparative diagnostic performances of Pittsburgh Compound B and ^{18}F-FDG in PET assessment of several subtypes of early cognitive impairment. . . . . ***Page 878***

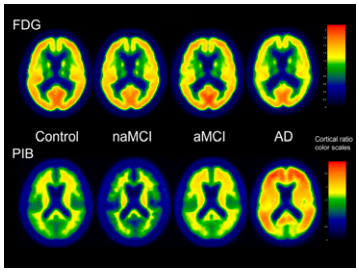

Antihistamines and cerebral H_1 receptors: Senda and colleagues use ^{11}C-doxepin PET to explore the effects of repeated administration of an antihistamine on the cerebral H_1 receptor and discuss resulting implications for PET in advancing new drug development. . . . . ***Page 887***

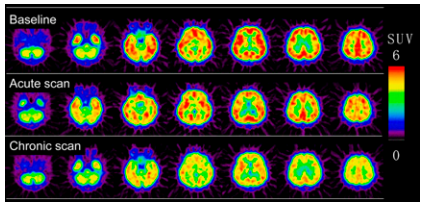

^{18}F-FDOPA PET in Parkinson disease: Jokinen and colleagues compare subregional striatal PET data from nonmedicated patients with early Parkinson disease and from healthy elderly volunteers to determine whether a simple ratio approach can reliably differentiate and identify early disease. . . . . ***Page 893***

PET and 5-HT$_4$ receptors: Marner and colleagues evaluate a technique for PET imaging and noninvasive quantification of serotonin-4 receptors using a novel ligand, ^{11}C-SB207145, and arterial input calculations. . . . . ***Page 900***

Identifying tracheal shine-through: Abdul-Fatah and colleagues describe a potentially confounding phenomenon resulting from the high energy and long range of positrons in ^{124}I PET/CT imaging in differentiated thyroid cancer. . . ***Page 909***

Skeletal muscle uptake of ^{18}F-6FDG: Spring-Robinson and colleagues evaluate the biodistribution of a nonphosphorylated glucose transport radiotracer for PET

imaging, with a focus on sensitivity to insulin stimulation. . . . . ***Page 912***

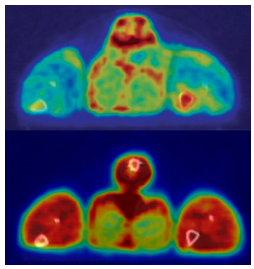

^{18}F-FDG uptake in RA: Matsui and colleagues report on in vitro and in vivo studies describing the correlation between ^{18}F-FDG accumulation and rheumatoid arthritis pathology and outline the potential for PET in quantifying inflammatory activity. . . . . ***Page 920***

Quantifying cell survival with ^{111}In: Blackwood and colleagues detail studies on cell labeling with ^{111}In for SPECT monitoring of transplanted cell viability in a canine myocardial infarction model. . . . . ***Page 927***

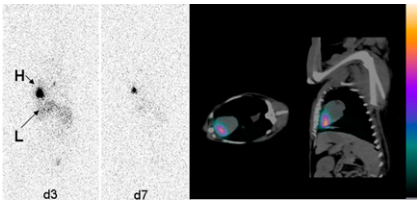

Internalization of sst$_2$ receptors: Waser and colleagues provide in vivo evidence of agonist-induced internalization of somatostatin-2 receptors and discuss the significance for targeted peptide receptor imaging of tumors. . . . . ***Page 936***

HIF-1 tumor hypoxia imaging: Kudo and colleagues assess the feasibility of a novel radiolabeled fusion protein, ^{123}I-POS, as an imaging probe for hypoxia-inducible factor-1, which plays a role in malignant tumor progression and resistance to radiotherapy. . . . . ***Page 942***

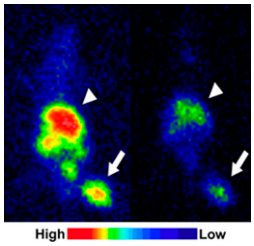

^{64}Cu-ATSM in muscles and tendons: Skovgaard and colleagues investigate exercise-related changes in oxygenation in rat skeletal muscles and tendons with hypoxia-selective ^{64}Cu-ATSM PET/CT and describe accompanying changes in gene expression of 2 hypoxia-related genes. . . . . ***Page 950***

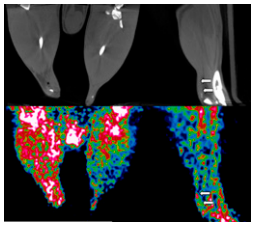

CT imaging of plaque inflammation: Hyafil and colleagues correlate the intensity of iodine-based contrast agent N1177 CT enhancement with ^{18}F-FDG PET/CT detection of inflammatory activity and histologic assessment of macrophage densityin a rabbit model of atherosclerosis. . . . . ***Page 959***

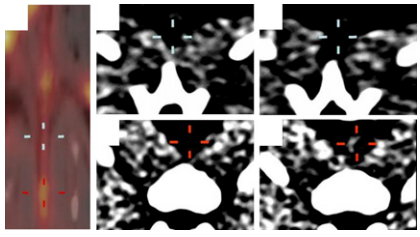

^{18}F-FDG rate constants in mouse brain: Yu and colleagues evaluate various methods for estimating the metabolic rate of glucose use in the mouse brain with small-animal PET and reliable blood curves derived by a microfluidic blood sampler. . . . . ***Page 966***

^{89}Zr-trastuzumab for HER2 immunoPET: Dijkers and colleagues describe the development of and comparative studies with a clinical-grade radiolabeled trastuzumab for HER2/*neu* immunoPET imaging, with applications in improved diagnosis, antibody-based therapy, and early antibody development. . . . . ***Page 974***

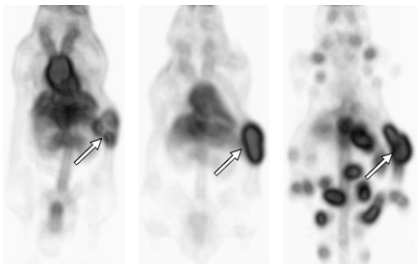

^{18}F-FAC PET in neuroinflammation: Marik and colleagues investigate the use of ^{18}F-FAC as a specific PET tracer of glial cell metabolism in rodent models of glioblastoma, focal ischemia, and ischemia–hypoxia. . . . . ***Page 982***

Radiolabeling using chelated Al-^{18}F: McBride and colleagues detail an efficient and easy method for radiolabeling a diverse array of molecules with ^{18}F for PET imaging. . . . . ***Page 991***

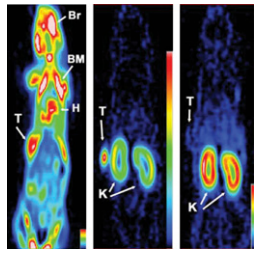

Nonradiolabeled molecular imaging: Gore and colleagues review the physical limitations of and potential opportunities for molecular imaging with MRI, CT, and ultrasound and point to the most promising areas for multimodal contrast agents. . . ***Page 999***

ON THE COVER

Peptide receptor imaging is based on agonist-induced internalization of peptide receptors in tumor cells. Compared with control rats (left), rats sacrificed at 2.5 min (middle) and 1 h (right) after TATE injection showed internalization of sst$_2$ in AR24J tumors on R2-88 immunohistochemistry. This molecular process is likely responsible for the uptake of sst$_2$ radioligands seen in vivo in sst$_2$-expressing tumors.

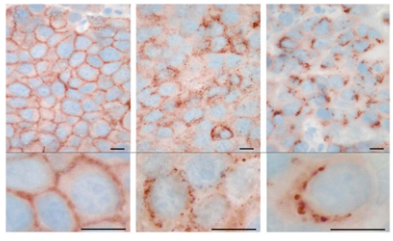

See page 940.